A KEY-POSE BASED REPRESENTATION FOR HUMAN ACTION RECOGNITION

A THESIS
SUBMITTED TO THE DEPARTMENT OF COMPUTER ENGINEERING
AND THE GRADUATE SCHOOL OF ENGINEERING AND SCIENCE
OF BILKENT UNIVERSITY
IN PARTIAL FULFILLMENT OF THE REQUIREMENTS
FOR THE DEGREE OF
MASTER OF SCIENCE

By
Mehmet Can Kurt
July, 2011

I certify that I have read this thesis and that in my opinion it is fully adequate, in scope and in quality, as a thesis for the degree of Master of Science.

Asst. Prof. Dr. Pınar Duygulu(Advisor)

I certify that I have read this thesis and that in my opinion it is fully adequate, in scope and in quality, as a thesis for the degree of Master of Science.

Asst. Prof. Dr. Selim Aksoy

I certify that I have read this thesis and that in my opinion it is fully adequate, in scope and in quality, as a thesis for the degree of Master of Science.

Prof. Dr. Aydın Alatan

Approved for the Graduate School of Engineering and Science:

Prof. Dr. Levent Onural
Director of the Graduate School of Engineering and Science

ABSTRACT

A KEY-POSE BASED REPRESENTATION FOR HUMAN ACTION RECOGNITION

Mehmet Can Kurt
M.S. in Computer Engineering
Supervisor: Asst. Prof. Dr. Pınar Duygulu
July, 2011

This thesis utilizes a key-pose based representation to recognize human actions in videos. We believe that the pose of the human figure is a powerful source for describing the nature of the ongoing action in a frame. Each action can be represented by a unique set of frames that include all the possible spatial configurations of the human body parts throughout the time the action is performed. Such set of frames for each action referred as “key poses” uniquely distinguishes that action from the rest. For extracting “key poses”, we define a similarity value between the poses in a pair of frames by using the lines forming the human figure along with a shape matching method. By the help of a clustering algorithm, we group the similar frames of each action into a number of clusters and use the centroids as “key poses” for that action. Moreover, in order to utilize the motion information present in the action, we include simple line displacement vectors for each frame in the “key poses” selection process. Experiments on Weizmann and KTH datasets show the effectiveness of our key-pose based approach in representing and recognizing human actions.

Keywords: Human motion, action recognition, key-pose, pose similarity, pose matching.

ÖZET

İNSAN HAREKETLERİNİN TANINMASI İÇİN ANAHTAR KARE TABANLI BİR POZ TEMSİLİ

Mehmet Can Kurt
Bilgisayar Mühendisliği, Yüksek Lisans
Tez Yöneticisi: Yrd. Doç. Dr. Pınar Duygulu
Temmuz, 2011

Bu tezde, videolardaki insan eylemlerini tanımak için anahtar kareye dayalı bir poz temsilinden faydalanılmaktadır. İnsan figürünün oluşturduğu pozun, bir kare içerisinde devam eden eylemi tanımlamak için çok güçlü bir kaynak olduğunu düşünüyoruz. Her eylem, o eylemin gerçekleştiği süre içerisinde insan vücudunun parçalarının oluşturduğu bütün uzamsal düzenleşimleri içeren bir kare grubuyla temsil edilebilir. "Anahtar Kare" olarak adlandırdığımız bu kare grubu bir eylemi diğerlerinden ayırt eder. "Anahtar Kare"leri seçmek için, insan figürünü oluşturan çizgilerle beraber bir şekil eşleme metodu kullanarak, verilen iki kare üzerindeki pozların arasında bir benzerlik değeri tanımlıyoruz. Bir kümeleme algoritması kullanarak, her eylemin benzer karelerini belirli bir sayıda kümede grupluyor ve bu grupların ağırlık merkezlerini "Anahtar Kare" olarak kullanıyoruz. Dahası, insan figürünü oluşturan çizgilerin hareketlerini video dizisi boyunca takip ederek, eylem içerisindeki devinim bilgisinden de faydalanıyoruz. Weizmann ve KTH verisetleri üzerinde elde ettiğimiz sonuçlar, "Anahtar Kare" bazlı yaklaşımımızın insan hareketlerini temsil etme ve tanımadaki etkinliğini göstermektedir.

Anahtar sözcükler: İnsan hareketi, eylem tanıma, anahtar kare, poz benzerliği, poz eşleme.

To my grandmother Aysel Tütüncü . . .

Acknowledgement

First and foremost, I would like to thank my supervisor Asst. Prof. Dr. Pınar Duygulu for her encouragement, guidance and kindness. She supported me in the best possible way throughout my studies.

I would also like to thank the members of my thesis committee Asst. Prof. Dr. Selim Aksoy and Prof. Dr. Aydın Alatan for reviewing my thesis and making valuable comments.

I would like to send my best wishes to my friend Sermetcan Baysal for sharing his ideas with me and for being such a great partner throughout my studies.

I thank my lovely wife, Pelin Damcı, for her amazing support during my seven years at Bilkent University. I am grateful to Gülçin Damcı, Nezih Damcı and Ayten Özbek for their incredible help and their love. I also would like to make a special reference to my best friend İlker Tufan for always being there for me.

Last but not least, I feel very lucky to have such a great mother and father, Gülay Kurt and Serdar Kurt, who have raised me with love and have supported me during my entire life. Without them, I couldn't be the person that I'm today.

Contents

List of Figures

Chapter 1

Introduction

1.1 Motivation

Human Action Recognition, which is a research area listed under computer vision, has drawn immense attention over the years. Previous research done in the field has resulted in a large variety of applications such as automatic surveillance and monitoring, social analysis and human-computer interaction. Along with the improving hardware technologies, the demanding nature of these applications keep the challenge of developing more effective and efficient systems for human action recognition alive.

Motivated by the needs of these applications, this thesis addresses the problem of recognizing human actions in videos automatically. However, it is well known that building a robust system for human action recognition is not trivial due to several reasons. First of all, finding the area of the image where the action is performed can be quite difficult. Especially, in cases where there is a great deal of noise in the background, spotting the human figure in its entirety is a challenging task. Secondly, even for simple actions, the way an action is performed may show a great variety from person to person. Moreover, the shooting conditions such as illumination changes in the environment, scale and viewpoint variations may cause further complications in the analysis of the ongoing actions. Considering these facts, representing the actions in a robust way plays an important role in the success of an action recognition system.

Despite the challenges for recognizing human actions explained above, the human brain can distinguish an action from the others just by looking at a single frame without having the need of seeing the rest of the sequence. This important observation is a clear indication of the fact that the pose formed by the human figure is a powerful source for describing an action. For this reason, exploiting the pose information encoded in a frame can be an effective approach in solving human action recognition problem. In fact, there are some previous studies [2, 3, 22], which attempt to represent the shape of a pose by using extracted human silhouettes. However, the performance of these works may suffer in the scenes where the quality of the extracted silhouettes are severely affected by the noise in the background.

An alternative approach for representing the pose information in a frame is to consider the pose of the human figure as a shape and to utilize one of the existing shape matching techniques in the literature of human action recognition. Shape Context Descriptor [1] introduced by Belongie et al. stands as a widely known shape matching technique which is initially developed as an object recognition scheme. In this thesis, we utilize Shape Context Descriptor as a tool to determine the similarity of the poses formed by the human figure in given frames. On top of identifying the pose differences in two actions by means of Shape Context, we extend the fact that the human brain can distinguish an action by looking at a single frame and we perform human action recognition by extracting a set of frames ("key frames") for each action.

This approach is powerful in distinguishing the actions which show significant differences in the poses the human figure forms. However,"key frames" might not be enough by itself to detect the differences between some actions such as walking and running. In order to get rid of such limitations, the pose representation might be supported by the motion information encoded in an action sequence. Therefore, in this thesis, we also maintain the motion information of the lines forming the human pose in each frame composing the "key frame" set.

1.2 Overview and Contributions

Our overall method consists of the following steps. Initially, we detect the lines in each frame of an action and hold a description for each line by using k-Adjacent Segments [8]. After applying some noise removal techniques, we come up with a set of lines which form the human figure in each frame. Secondly, we generate a set of uniform points from the extracted lines. By feeding these points into Shape Context [1], we generate a descriptor vector for each point in the frame. The generated descriptors for each point are combined into a Shape Context matrix.

Thirdly, in order to find the similarity value between a pair of frames of an action, we calculate the distance between the shape context descriptors of each pair of points in the frames by means of chi-square distance. We create a similarity matrix with the computed distance values and produce a matching between the points of the frames with one of the two methods; Left-To-Right Matching or Hungarian Method [14]. Based on two different strategies, Left-To-Right matching and Hungarian Method have their own advantages which may reveal in different cases. For a more accurate matching between the points, we also employ a spatial constraint which prevents any two points that are located in different regions of the frames from being matched. After creating a set of matched points, we compute an overall similarity value between two frames by using the individual similarity values between matched points.

As a next step, we group the similar poses of each action in a defined number of clusters by using k-medoids clustering algorithm and we form the “key frame” set for that action by taking the medoid of each cluster.

In order to support the “key frame” set of each action with motion information, we detect the location of the lines forming the human figure in a key frame in the frames that come just before and right after it. After spotting each line both in previous and next frame, we calculate a displacement vector for that line by taking the difference in x and y coordinates. This displacement information reflects where the line is coming from and where it is going next. Repeating this process for each line in the key frame, we create two displacement vectors that we call “from where” and “to where”. This step completes the entire training process.

For classifying a given sequence of poses, we utilize three schemes; Majority Voting, Sum of Minimum Distance and Dynamic Time Warping. When using the Majority Voting, we compare each frame of the test sequence to all key frames of all actions and assign the action label of the most similar key frame to that frame. Repeating the same procedure for the entire test sequence, we apply Majority Voting among the assigned labels in order to make a final decision. On the other hand, when using the Sum of Minimum Distance, we find each action’s most similar key frame to each test frame and we accumulate those minimum distances. Finally, the label of the action that has the minimum total distance becomes the classification result of the tested sequence. When using the Dynamic Time Warping (DTW), we find a correspondence between the pose order of two sequence. Calculating a similarity value between the given test sequence and training sequences of each action, we classify the test sequence as the action that contains the most similar training sequence with respect to DTW distance.

We present two important contributions with this thesis. The first one is approaching the human action recognition as a shape matching problem and applying Shape Context, which is developed for object recognition, for recognizing human actions. The second is representing an action with a set of frames named as “key frames” which cover the pose information in an action sequence along with the motion information.

1.3 Organization of the Thesis

The remainder of this thesis is organized as follows.

Chapter 2 presents a literature review in human action recognition. It describes the previous work done in the field and discusses its drawbacks.

Chapter 3 describes our approach. It explains our key-frame extraction algorithm in detail and shows how actions can be classified by utilizing the extracted key-frames.

Chapter 4 shows the experiments conducted on the state-of-the-art action recognition datasets, discusses our results and compares them with the results of the previous work.

Finally, Chapter 5 shows our concluding remarks and introduces possible future research.

Chapter 2

Related Work

Human Action Recognition has received considerable attention over the last decade. There are a large number of recent studies which approach the problem in different ways. In this chapter, we give a review of the previous work performed in the field.

2.1 Review of Previous Studies

A large number of studies in the past extend 2D interest points used in object recognition and apply the idea to the spatio-temporal case. In [15], by employing a space-time extension of Harris operator, Laptev et al. detect interest points in multiple levels of spatio-temporal scales and use them for action recognition by employing a SVM classifier. Dollar et al. in [5] combine space-time interest point approach with bag of words model which is often employed in information retrieval. They represent an action by a statistical distribution of the bag of video-words after extracting interest points by applying separate linear filters in both spatial and temporal directions. In [17], Liu et al. give a a model in which they quantize the extracted 3D interest points and represent a video sequence by a bag of spatio-temporal features named as video-words. In the same work, they discover the optimal number of video-word clusters by means of Maximization of Mutual Information. Bag of words model discards the temporal order among features. However, this ordering information often contains quite important information about the nature of the action. For instance, sit down and get up actions, which are performed by the same set of body movements but just in different directions, can be easily distinguished from each other by a representation which preserves the temporal ordering between the features. Nowozin et al. in [21] emphasize this observation and present a sequential representation which retains the temporal order.

A recent trend in action recognition has been the emergence of methods that treat a sequence of images as three-dimensional space-time volume. Qu et al. in [22] take a sequence of full silhouette frames as input and generate a global feature by extracting the differences between frames. Considering human actions as three-dimensional shapes, Blank et al. in [2] extract space-time features such as local space-time saliency, action dynamics, shape structure and orientation. Both of these studies make the assumption that input silhouettes contain detailed information about the pose of the human figure. However, in cases where there is an absence of static cameras and a good background model, obtaining such silhouettes can be problematic. One study that emphasizes this subtle point is [13]. In this work, without the need of any background subtraction, Ke et al. segment input video into space-time volumes and correlate action templates with the volumes using shape and flow features.

Another group of works can be categorized as optical flow based approaches. Efros et. al. in [6] introduce a motion descriptor based on optical flow measurements by treating optical flow as a spatial pattern of noisy measurements instead of precise pixel displacements. Wang et al. in [28] exploits optical flow in conjunction with bag of words approach. After computing optical flow at each frame of a video sequence, they run k-medoids clustering on a similarity matrix where each entry is the similarity between two frames calculated using a normalized correlation on optical flow features and generate codewords. Yet another work that uses optical flow is [7]. In this study, Fathi et al. first extract the low-level optical flow information and construct mid-level motion features on top of them by using the AdaBoost training algorithm. Flow-based approaches are invariant to appearance variations and they work without the need of any background subtraction. However, the likelihood to have similar flows in many scenes over short periods of time stand as a main downside.

In addition to the previous three approaches, shape-based methods, which exploit the pose of the human figure in an action sequence, have also been studied widely. İkizler et al. in [12] represent each human pose in a sequence by fitting oriented rectangular patches over the body and generating a bag-of-rectangles descriptor. In a similar work [10], Hatun et al. describe the poses with histogram of oriented gradients (HOG) features. In contrast to previous study, they preserve the temporal characteristics of actions by representing videos as ordered sequence of pose-words and employing string matching techniques on them for classification. Another study that utilize the temporal ordering of features is [26]. In this work, Thurau et al. extract HOG features and employ the n-gram model when creating histograms.

A group of studies in shape-based approaches focus on representing the actions as a set of key poses. Carlsson et al. in [4] recognize the action in a video sequence by matching shape information in the frames to stored prototypes that represent key frames of an action. Their shape matching algorithm is based on estimating the deformation of the shape in the image to the shape of the stored prototype. In contrast to this work, which selects only a single key-frame for each action by manual inspection, Loy et al. in [19] present a method for automatic extraction of the key frames from an image sequence. After following the same shape matching scheme in [4], they divide the sequence into clusters of frames by using an extended version of the normalized-cut segmentation technique and use the central frame of each cluster as key-frames.

Although most of the shape-based approaches show very promising results, distinguishing some actions such as running and walking from each other might be very difficult since generally the human poses in these actions look very similar. In these cases, discarding dynamics of the motion in the action is intolerable. Therefore, in order to remove this shortcoming of shape based approaches, some previous studies use shape and flow features in a complementary manner. Lin et al. in [16] learn action prototypes in a joint feature space by capturing the correlations between shape and motion cues and they perform recognition via tree-based prototype matching. İkizler et al. in [11] represent human actions by using line and optical flow histograms. As shape feature, they extract a histogram which reflects the spatial distribution and characteristics of lines fitted to boundaries of human figures. They combine the computed shape features by motion information that they capture with a slightly modified version of the optical flow.

2.2 Discussion of Related Studies

Most of the studies, that use shape information alone or combined with the motion information, extract shape features by employing histograms of rectangles, lines or gradient values. Even though some of these approaches impose a level of localization by dividing the image into equal-sized bins, they still miss the spatial relation information between the individual components of the human bodies. In this thesis, to encode the pose information, we utilize the shape representation in [1] developed originally for object-recognition. We think that this shape representation describes the human shape in more detail since it also captures the relative positioning of the limbs that define the nature of an action.

The main drawback of the aforementioned studies that employ stored pose prototypes for recognition is the lack of information about the motion. In these studies, a global motion information is hard to be involved in the overall process, since the classification is performed on a frame-by-frame basis. In this thesis, we address this shortcoming by incorporating the motion information in the key frame extraction step. For each key frame, we maintain two motion features which correspond to the general displacement of the lines forming the human figure in that key frame. We believe that supporting the pure key frames even with that small level of motion clues affect the recognition performance considerably.

Chapter 3

Our Approach

In this chapter, we present our approach for classifying human actions. First, we give the details of our pose extraction and representation scheme (Section 3.1). Second, we present the method to calculate the similarity between two given frames (Section 3.2). Next, we show how we find a set of representative frames for each action (Section 3.3). Then, we explain how we introduce a level of motion information to the key frame selection process (Section 3.4). Finally, we describe the classification methods that we exploit for labeling a given set of frames with one of the available actions (Section 3.5).

3.1 Pose Extraction and Representation

3.1.1 Line Extraction

Since our approach depends on the pose information, our ultimate interest is in the shape formed by salient parts of the human body. In order to extract the shape of the human pose, we utilize the points forming the boundary of the human figure in the image. For achieving this goal, there exist two alternatives; detecting the points of interests and sampling among them in a uniform manner or detecting the lines in the given frame and sampling points from the detected

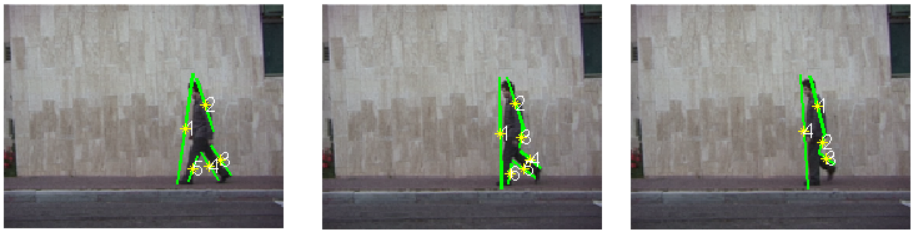

Figure 3.1: This figure shows the extracted lines on a set of consecutive frames from a walking sequence. Extracted lines are shown in green. Center points of the lines are numbered and shown as yellow stars.

lines. We argue that the second approach gives a more consistent and meaningful set of points. Therefore, the very first step in our action recognition mechanism is the extraction of lines in a given frame.

In order to find the lines in a given frame, we use the line descriptor introduced by Ferrari et al. in [8]. Accompanied by a user-defined edge detection scheme, this algorithm produces a set of lines in each given frame along with the following descriptor for each line;

$$V_{line} = (id, c_x, c_y, \theta, l, s) \tag{3.1}$$

Here, id refers to a unique identification number for each line in the given frame, c_x and c_y are the coordinates of the center of the line, θ is the orientation of the line which ranges from 0 to 2Π, l is the length of the line and s is the average strength of the edges composing the line. In our approach, we often utilize c_x and c_y information of each line.

3.1.2 Shape Context Descriptor

In order to represent the pose information in a given frame, we use the well-known shape context descriptor introduced by Belongie and Malik in [1]. Shape context measures the shape similarity of a given pair of images by finding a match between the points contained in the images. So far, shape context descriptor has been generally employed for the purpose of object recognition. However, in this

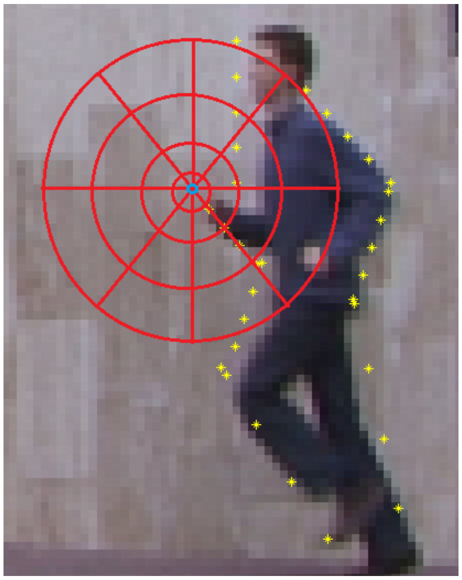

Figure 3.2: This figure demonstrates the shape context calculation process. In shape context, a circular grid is positioned over the sample points of an image and a histogram SC with size $r \times u$ is generated for each point where r is the number of radial bins and u is the number of orientation bins.

work, we show that we can make use of it for human action recognition as well.

Shape context works as follows; first, a set of points $P = \{p_1, p_2, p_3, ..., p_n\}$ is sampled from the exterior or interior contours on the object in the image. One important note to indicate here is that this set of points should not necessarily be curvature or maxima points. Next, a circular grid, which has r radial and u orientation bins, is centered at each sampled point p_i. For each point p_i, a histogram with size $r \times u$ is generated and each cell of that histogram is filled with the total number of points which are positioned at the corresponding bin location relative to point p_i. The shape context for point p_i can be defined as the coarse distribution of the relative coordinates of the rest of the $n-1$ points with respect to p_i. Repeating this procedure for each sampled point, a matrix SC with n rows and $r \times u$ columns is generated for each image. In Figure 3.2, an example grid is shown on a frame that belongs to a running sequence.

After computing the shape context, one can utilize various similarity distances to find the similarity between two points. In [1], Belongie et al. suggest that chi-square distance can be used for this purpose. According to that, given two frames

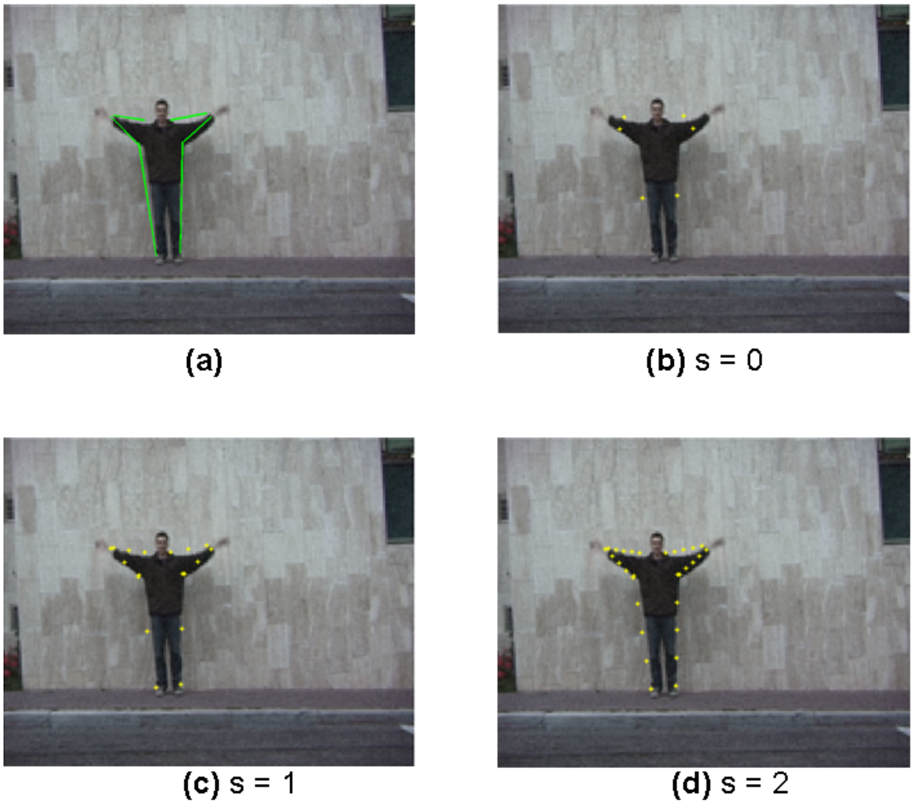

Figure 3.3: This figure illustrates the effect of increasing the sampling factor on generated set of points. (a) shows the extracted lines on the human figure. (b) shows the set of generated points (only the center points) when sampling factor is 0. (c) illustrates the generated points when sampling factor is 1. Generated points contain both the center points and the two end points of each extracted line. (d) illustrates the generated points when sampling factor is 2. The shape of the human figure is represented in detail.

f_1 and f_2, the similarity between the shape context descriptors SC_{1i} and SC_{2j} of the points p_i in f_1 and p_j in f_2 can be calculated by using chi-square distance X^2 as follows;

$$X^2\left(p_i, p_j\right) = \frac{1}{2}\sum_{k=1}^{N}\frac{\left(SC_i\left(k\right) - SC_j\left(k\right)\right)^2}{SC_i\left(k\right) + SC_j\left(k\right)} \tag{3.2}$$

3.1.3 Point Generation

Feeding the shape context algorithm with a good set of points is a crucial step for the accurate representation of the actions in the images. For this purpose, we utilize the line detection algorithm indicated in Section 3.1.1. We store the main properties of all the detected lines such as the coordinates c_x and c_y of the center point, the length l and the orientation θ. One approach for point generation is just to take the center point of each line and to feed these points to shape context calculation process. Our experiments show that merely using center points is inadequate for a detailed representation of the pose. Therefore, alternatively, by making use of length and orientation information, we generate the endpoints of each line and pass these generated points to the shape context calculation process. Clearly, generating 3 points from each line would give us a better pose representation. In fact, this approach can be generalized so that we can sample as many points as we want from a single line. In our experiments, we will define sampling parameter as s and show the effects of increasing s on the results. Figure 3.3 illustrates the effect of increasing s on the generated set of points.

3.2 Finding Similarity between Two Poses

We can calculate the similarity value between the poses contained in a pair of frames f_1 and f_2 by utilizing shape context descriptors in the following steps;

1. After extracting the lines on each frame and generating points from those lines, we calculate the shape context descriptors SC_1 for f_1 and SC_2 for f_2 as described in Section 3.1.2.
2. Then, we create a similarity matrix SM_{sc} which holds the similarity distance between each pair of points from f_1 and f_2. The similarity between any two points can be calculated using Formula 3.2.
3. Next, we match each point in frame f_1 to another point in frame f_2 by

using the calculated distances in matrix SM_{sc}. Here, different matching strategies can be employed. We present different matching strategies in the next section.

4. The overall distance between frames f_1 and f_2 can be calculated by using Formula 3.3 or 3.4.

3.2.1 Matching Methods

We can use different strategies to find matches between the points of two frames by using their shape context similarity values. Since the overall similarity value between two frames depends on the quality of the matching between the points, this step has a direct impact on the accuracy of the recognition results.

3.2.1.1 Left-To-Right Matching

One strategy that can be followed for matching is to match each point in f_1 to the most similar point (the point that has the lowest similarity distance value) in f_2. If this approach is utilized, there is a high chance that more than two points in f_1 will be matched to the same point in f_2. In order to prevent this situation, we introduce a constraint which guarantees that a point p_i in frame f_1 can be matched with point p_j in frame f_2 if and only if;

- among all points in frame f_2, p_j is the most similar point to p_i, and
- among all points in frame f_1, p_i is the most similar point to p_j.

We can consider the points in frames f_1 and f_2 being the elements of two different sets P_1 and P_2, respectively. This constraint assures that each element in set P_1 can be associated with exactly one element in set P_2. We call this strategy **Left-To-Right Matching**. Figure 3.4 illustrates an example matching between two frames by using this strategy.

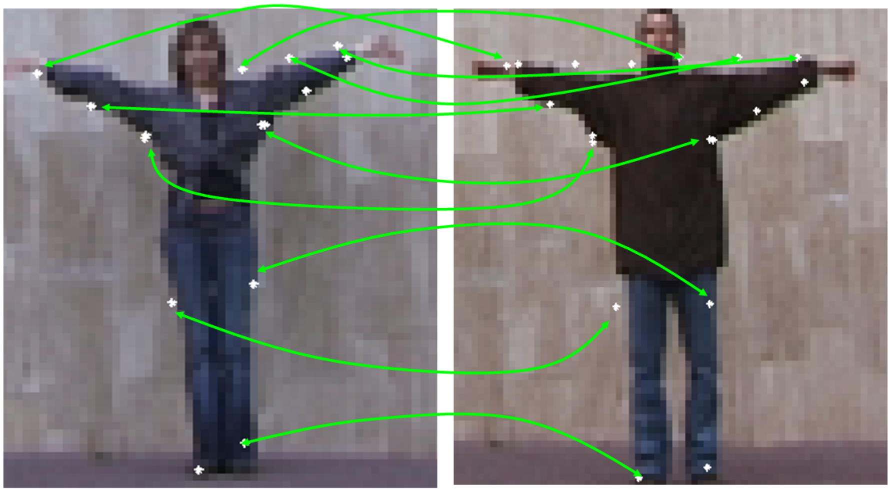

Figure 3.4: This figure shows a set of matched points between two frames belonging to wave action when Left-To-Right matching is used. Matched points are connected with green lines.

Once the points in frames f_1 and f_2 are matched by Left-to-Right matching strategy, we employ Formula 3.3 to calculate an overall similarity value.

$$sim\left(f_1, f_2\right) = \frac{\sum_{i=1}^{|M|} d(M_i)}{|M|} + penalty \times \frac{max\left(\left|P_1\right|, \left|P_2\right|\right) - |M|}{max\left(\left|P_1\right|, \left|P_2\right|\right)} \tag{3.3}$$

Here, we denote the set of matching points as M. Each M_i, where i ranges from 1 to $|M|$, represents a pair of matched points, one point belonging to P_1 and the other point belonging to P_2. We denote the similarity distance between the points in matched pair i as $d\left(M_i\right)$. The first term and second term in the formula measure two different aspects for expressing the overall similarity between frames f_1 and f_2. The first term in the formula is the average of the similarity distances between the matched points in M and it basically reflects how similar the shapes of the human pose contained in frame f_1 and f_2 are. On the other hand, the second term introduces an additional factor to the overall similarity by multiplying the percentage of the number of unmatched points with a predefined constant referred as *penalty*. We believe that representing similarity and dissimilarity of the shapes in f_1 and f_2 in such a combined fashion gives us a more accurate comparison.

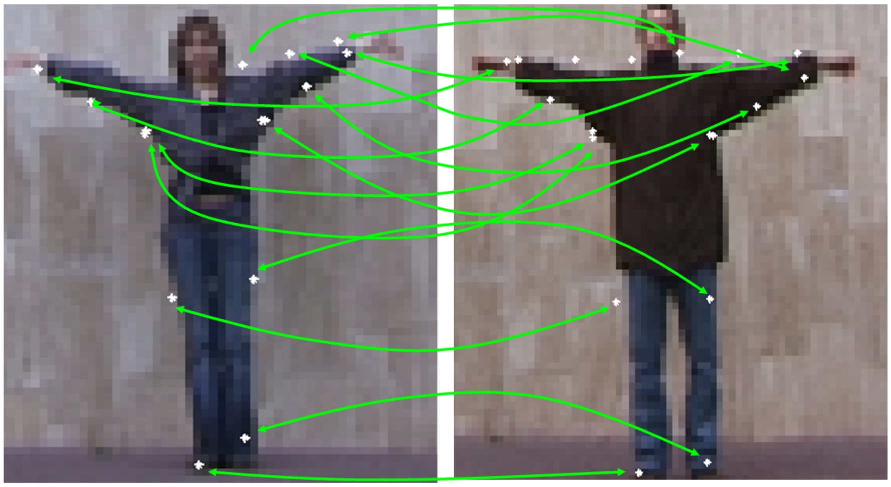

Figure 3.5: This figure illustrates another set of matched points between the same frames in Figure 3.4 when Hungarian Method is used. Matched points are connected with green lines.

3.2.1.2 Hungarian Method

An alternative matching method is the algorithm used in [1]. **The Hungarian Method** is a combinatorial optimization algorithm and it gives the matching between the elements of two sets that has the minimum total cost. Hungarian Method is different from Left-To-Right Matching in the sense that it may not match a point to its counterpart right away. Instead, it produces a matching in which the global similarity distance summation is minimized. The details of this matching scheme can be found in [14]. Figure 3.5 illustrates an example matching between two frames by using the Hungarian Method.

$$sim\left(f_1, f_2\right) = \frac{\sum_{i=1}^{|M|} d(M_i)}{|M|} \tag{3.4}$$

Hungarian Method provides a *one-to-one* and *onto* matching, in which each and every element in P_1 is associated with exactly one element in P_2. Since each point in set P_1 has a corresponding point in set P_2, the second term in Formula 3.3 becomes inapplicable when Hungarian Method is in use. Therefore, in this case, we employ Formula 3.4.

3.2.2 Utilizing Other Visual Clues

As indicated previously, similarity matrix SM_{sc} holds the shape context similarity between each pair of points in given frames f_1 and f_2. Both Left-To-Right matching and Hungarian Method operate on SM_{sc} and generate a set of matched points. In order to calculate the similarity between points, one can utilize other visual clues along with the shape context descriptor. It is observed that combining these clues together with the shape context usually results in more accurate matches and consequently higher recognition rates.

In our work, we know the orientation θ of each line which originates our sample points. We define the orientation distance between any two points p_i and p_j by using Formula 3.5. Here, θ_i and θ_j denote the orientation values of the lines where the points i and point j originate from.

$$d_\theta(i, j) = \frac{|\theta_i - \theta_j|}{\pi/2} \tag{3.5}$$

By finding the orientation similarity between each pair of points, we generate a similarity matrix SM_θ. We can make use of the orientation similarity in the point matching process by adding SM_θ to SM_{sc} and letting the matching strategy operate on the resulting matrix. In fact, this approach can be generalized by introducing other visual clues and taking a weighted combination of them as depicted in Formula 3.6. In the experiments section, we show how using different weights affect the overall recognition performance.

$$SM = \alpha_{sc} \times SM_{sc} + \alpha_\theta \times SM_\theta + \alpha_x \times SM_x + \ldots \tag{3.6}$$

3.2.3 Spatial Binning

An important constraint that can be exploited during the matching process is the locations of the generated points in the image. For example, matching a

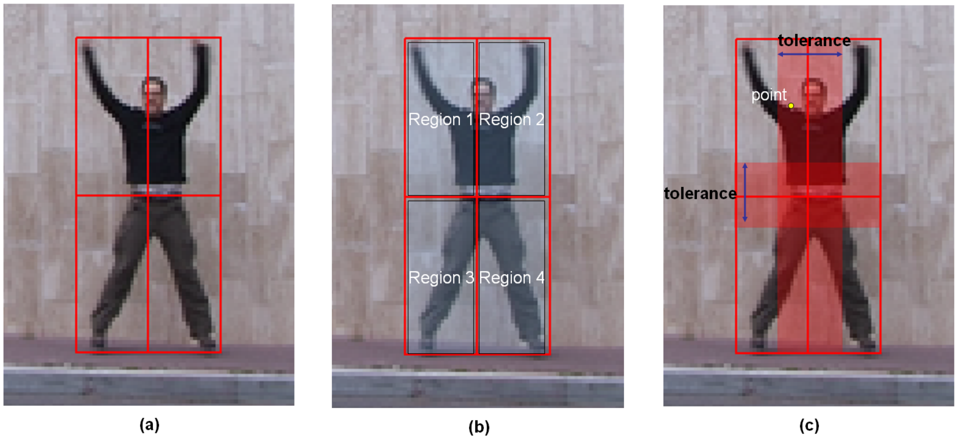

Figure 3.6: This figure illustrates the spatial binning applied to a human pose. Spatial binning approach can be generalized to any N X N binning. In this work, we use N as 2, which results in 2 X 2 spatial binning as shown in **(a)** and **(b)**. **(c)** illustrates the tolerance value we define on spatial binning. Points in red shaded transparent rectangles are the ones which are affected by the tolerance value. For example, the point shown in small yellow circle is considered as belonging to both Region 1 and Region 2.

point lying on an upper body contour to a point lying on a lower body contour is not meaningful even if they have similar shape context descriptors. In order to guarantee that no two points located on different parts of the human contour can be matched, we first divide the human figure represented in a given frame into 4 bins such as *upper body left*, *upper body right*, *lower body left* and *lower body right*. During the matching process, allowing the points to be matched only if they come from the same bin region ensures this constraint. Figure 3.6 illustrates dividing the human figure in an image into four bins. Clearly, this constraint can be generalized into any $N \times N$ binning.

When dividing a given frame into any $N \times N$ bin regions, we first calculate the range of x and y coordinates of the points forming the human figure. Then, we divide both ranges into N equal pieces. Drawing horizontal and vertical lines which intersect the division points seperating these pieces gives us a $N \times N$ grid on the human figure. During the calculation of the boundaries that define a bin region, it is likely to have some offsets in the x and y coordinates because of the unsymmetrical shape of the human pose and/or imperfect edge detection results. Such shifts may lead to some points to be contained in bin regions where they do not belong.

In order to deal with this problem, we define a tolerance value on the spatial binning. According to that, if a sample point is within a certain pixel distance to the boundary that divides two bin regions, we consider that point to be contained in both of them. Again, Figure 3.6 illustrates the tolerance value and its effect on a point in the given example frame.

3.3 Finding Key Frames

Our approach presented in this thesis depends on the *key frames* we extract from the available video sequences of each action. We define *key frames* as a set of frames that uniquely distinguishes an action from others. Intuitively, to find key frames, it is reasonable to group the frames which show common pose appearances. Thus, we base our key frame extraction process on the k-medoids clustering algorithm.

For each action a_i consisting of n frames such as $\{f_1, f_2, \ldots, f_n\}$, a set of key frames KF_i with size K can be found as follows; first, a similarity matrix SM_{frm} is created by means of Formula 3.3 or Formula 3.4, depending on the choice of point matching strategy. Every element $SM_{frm}(j, k)$ corresponds to the similarity between frame f_j and f_k. Then, similarity matrix SM_{frm} is given as the input to k-medoids clustering algorithm. k-medoids partitions the frames $\{f_1, f_2, \ldots, f_n\}$ into K clusters, where cluster medoids are $\{KF_{i1}, KF_{i2}, \ldots, KF_{iK}\}$. Since the cluster medoids tend to represent common poses in each action, we define the cluster medoids as the key frame set KF_i for action a_i. As the work in [24] indicates, simple human actions can be classified almost instantaneously. In most cases, using a very short sequence (1-10 frames) of key frames for each action is enough to classify actions successfully. In our experiments, we keep the number of representatives for each action as small as possible. On the other hand, we

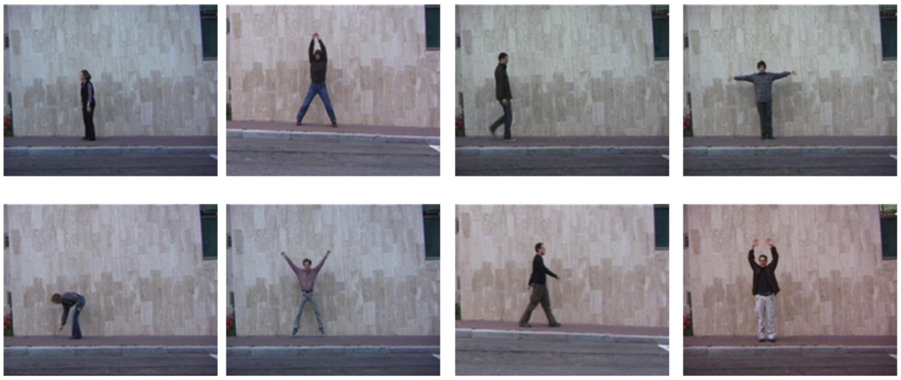

Figure 3.7: This figure shows two extracted key frames for actions bend, jack, walk and wave presented in Columns 1 to 4, respectively.

observe that there are some factors which may result in a certain increase in the number of required representatives for accurate classification. One example of such factors is the actors performing a particular action in different ways. Moreover, the viewpoint and zoom factor of the camera can be listed as other factors that have an affect on the number of key frames. We believe that increasing the number of representatives to a certain point resolve such issues in most cases. In the experiments section, we show the effects of K on the recognition performance. Figure 3.7 illustrates the key frames that are extracted by our approach for two different actions.

3.4 Utilizing Motion Information

Pose information itself is powerful enough to recognize most of the actions. However, ignoring the motion information encoded in an action sequence might be intolerable when distinguishing actions such as walking and running which contain similar pose appearances. Unfortunately, it is hard to involve a global motion information in key frame based approaches, since the classification is performed generally on a frame-by-frame basis. In order to deal with this shortcoming, we associate two displacement vectors with each frame and introduce a level of motion information in the key frame selection process. These vectors, which we name as fw ("from where") and tw ("to where"), reflect the general displacement of the points in a frame with respect to their positions in previous and next frame.

For a frame f_i, we extract $f\vec{w}_i$ vector in the following steps; first, we initialize $f\vec{w}_i$ with all zeros. $f\vec{w}_i$ consists of 4 nonnegative components $\left\{fw_i^{+x}, fw_i^{-x}, fw_i^{+y}, fw_i^{-y}\right\}$ which represent magnitude of the total displacement of the points in $+x, -x, +y$ and $-y$ directions, respectively. Then, we generate points on the human contour of frames f_{i-1} and f_i as described in Section 3.1.3. Next, by using the same point matching techniques explained in Section 3.2, we find corresponding matches between points of f_{i-1} and f_i. Let (p_j, p_k) be a matched pair of points, where p_j lies on f_{i-1} and p_k lies on f_i. We calculate the displacement in x and y coordinates of these points with Formula 3.7.

$$\begin{aligned} x_{diff} &= x_{i-1,j} - x_{i,k} \\ y_{diff} &= y_{i-1,j} - y_{i,k} \end{aligned} \tag{3.7}$$

After calculating the displacement in x and y coordinates, we accumulate the computed difference to the corresponding cell of $f\vec{w}_i$ vector. For instance, if x_{diff} is a positive value, we add $|x_{diff}|$ to fw_i^{+x}. Otherwise, we add $|x_{diff}|$ to fw_i^{-x}. We update fw_i^{+y} or fw_i^{-y} in the same fashion depending on the sign of y_{diff}. Repeating the same procedure for each matched pair of points results in $f\vec{w}_i$ which provides a level of motion information with respect to the previous frame.

We extract $t\vec{w}_i$ vector in a similar fashion. This time, instead of matching the points with f_{i-1}, we match the points of f_i with next frame f_{i+1}. As described previously, we calculate the displacement magnitudes for each matched pair of points and accumulate those values in $t\vec{w}_i$ vector. Figure 3.8 gives a feel of this process by illustrating the counterpart of a point in the previous and next frames and shows the displacement vectors for a single point.

There are multiple ways to integrate the extracted motion information into the key frame selection process. In section 3.2.2, we emphasized that combining other visual clues together with the shape context descriptors results in more accurate measurements in defining the similarity between points. Moreover, in Formula 3.6, we showed how we can obtain a weighted combination of the similarity values

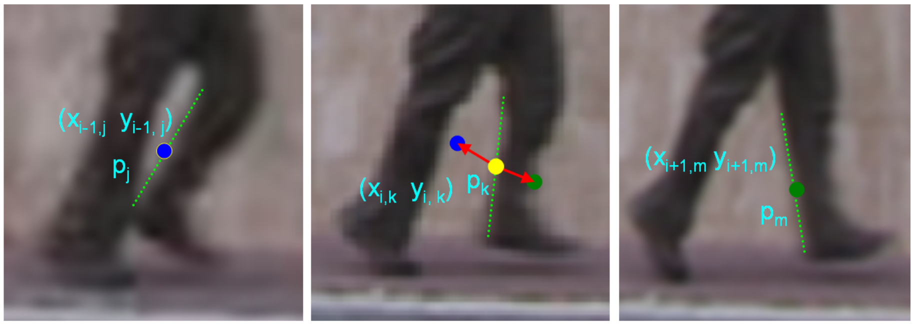

frame i - 1 frame i frame i + 1

Figure 3.8: This figure shows the displacement vectors (drawn in red in middle frame) for the yellow point p_k in the middle frame i. The point p_j is the counterpart of p_k in previous frame i - 1 whereas the point p_m is its counterpart in next frame i + 1. The red line going from yellow point to blue point shows where the yellow point is previously whereas the red line going from yellow point to green point shows where it goes next. fw and tw vectors described below are composed by accumulating the individual displacement vectors for each matched point.

coming from different clues and produce an overall similarity matrix. We can extend formula 3.6 in order to introduce motion information which are represented by fw and tw vectors. We calculate the similarity between any two fw and tw vectors by employing chi-square distance X^2. Thus, the new formula becomes the following;

$$SM = \alpha_{sc} \times SM_{sc} + \alpha_{\theta} \times SM_{\theta} + \alpha_{fw} \times X^2(fw_i, fw_j) + \alpha_{tw} \times X^2(tw_i, tw_j) \quad (3.8)$$

As an alternative to incorporate motion information right into similarity matrix, we can integrate the constants coming from $X^2(fw_i, fw_j)$ and $X^2(tw_i, tw_j)$ in Formula 3.3 and 3.4. If this alternative approach is to be adopted, these formulas take the following forms, respectively;

$$sim\,(f_1, f_2) = \frac{\sum_{i=1}^{|M|} d(M_i)}{|M|} + penalty \times \frac{max\,(|P_1|\,, |P_2|) - |M|}{max\,(|P_1|\,, |P_2|)} + X^2(fw_i, fw_j) + X^2(tw_i, tw_j) \quad (3.9)$$

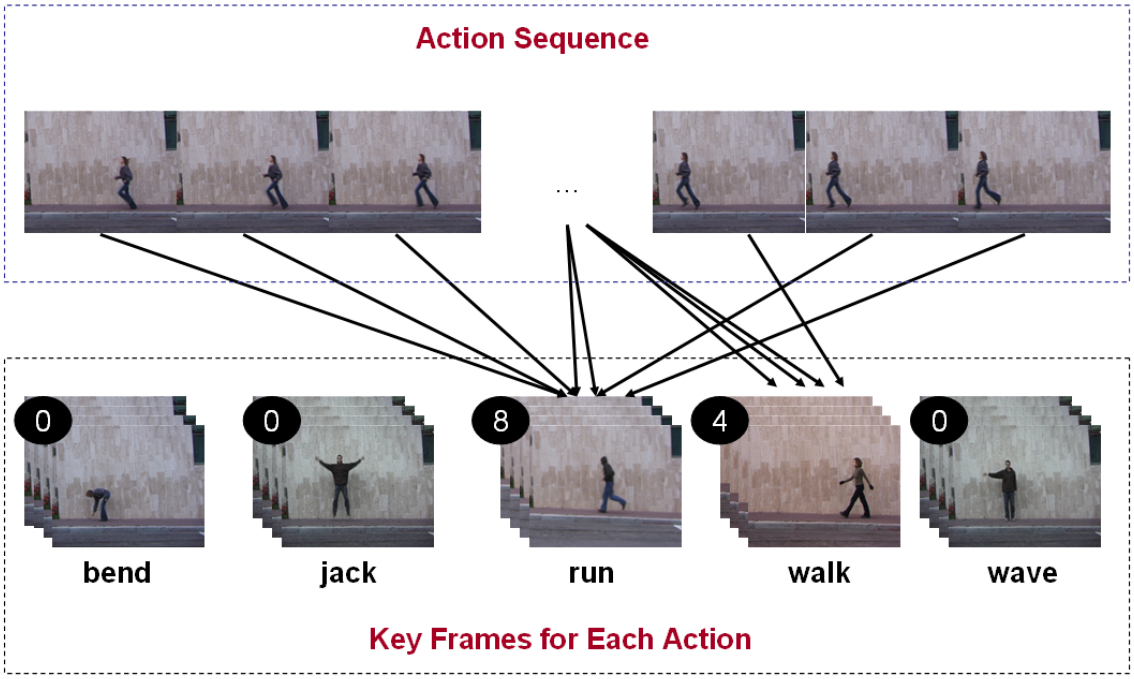

Figure 3.9: This figure demonstrates action recognition using Majority Voting classification scheme. The given sequence is classified as "run" with 8 votes.

$$sim\,(f_1, f_2) = \frac{\sum_{i=1}^{|M|} d(M_i)}{|M|} + X^2(fw_i, fw_j) + X^2(tw_i, tw_j) \tag{3.10}$$

3.5 Recognizing Actions

In order to classify a given action sequence, we use three different classification techniques; *Majority Voting*, *Sum of Minimum Distances* and *Dynamic Time Warping*.

3.5.1 Majority Voting

Majority Voting can be described as a frame-by-frame basis comparison approach. Given an action sequence consisting of frames $\{f_1, f_2, f_3, \ldots, f_n\}$, for each frame f_i, we first compute the similarity values $d_j(i, k)$ between f_i and all of the frames

KF_{jk} in key frame set $KF_j = \{KF_{j1}, KF_{j2}, KF_{j3}, ..., KF_{jK}\}$ where j represents an action in the available action set $\{a_1, a_2, a_3, \ldots, a_m\}$ and K is the number of key frames for each action.

Next, we find the minimum of $d_j\,(i,k)$ for all j and k and assign f_i the action label j which contains the minimum similarity value $d_j\,(i,k)$. In other words, we apply a 1-NN classifier to f_i and assign the action label of the nearest key frame of all actions. Equation 3.11 describes this step in formal notation.

$$\textbf{arg min}_j\; d_j\,(i,k) \quad \forall j\; 1 \leq j \leq m \text{ and } \forall k\; 1 \leq k \leq K \tag{3.11}$$

While labeling each frame in the same way, we keep a vector $V = \{V_1, V_2, V_3, \ldots, V_m\}$ which holds the number of frames assigned to each action. Once all the labeling is done, we compare the values in V and classify the sequence $\{f_1, f_2, f_3, \ldots, f_n\}$ as the action that has the maximum number of votes. This step is formulated in Equation 3.12. Moreover, Figure 3.9 illustrates classification of a sequence with Majority Voting.

$$\textbf{arg max}_c\; V_c \quad \forall c\; 1 \leq c \leq m \tag{3.12}$$

As an alternative to 1-NN classifier used for assigning an action label to a frame, we can employ 3-NN classifier which we believe provides more accurate results. While using 3-NN, we find the nearest three neighbours of each frame f_i. If any two of the three neighbours (key frames) belong to the same action j, we assign f_i action label j. However, if all of the three neighbours are contained in key frame sets of different actions, we exclude frame f_i from the classification process. In the experiments section, we compare 1-NN and 3-NN and show which one is superior over the other.

3.5.2 Sum of Minimum Distances

During our analysis, we observe that the poses in some key frames of different actions may be very similar. For example, walking and running actions in Weizmann dataset [9] share instances where it is very difficult to differentiate the two actions from each other just by looking at the pose information in the figures. Similarly, handclapping and handwaving actions in KTH dataset [25] contain some frames where the human figure is facing the camera with arms sticking to the body. Majority Voting labels such frames with the action which has the most similar key frame. Therefore, when classifying a handwaving sequence, a large number of frames can be labeled as handclapping. This clearly results in a decrease in the recognition performance.

In order to minimize the effects of such common poses, we make use of the Sum of Minimum Distances classification scheme. Given an action sequence consisting of frames $\{f_1, f_2, f_3, \ldots, f_n\}$, for each frame f_i, we again compute the similarity values $d_j(i,k)$ between f_i and all of the frames KF_{jk} in key frame set $KF_j = \{KF_{j1}, KF_{j2}, KF_{j3}, ..., KF_{jK}\}$. (We use the same notation in Section 3.5.1)

Instead of using a k-NN classifier for labeling f_i right away, we find the minimum $d_j(i,k)$ for each action j and accumulate those distances within a seperate vector $MD = \{MD_1, MD_2, MD_3, \ldots, MD_m\}$. Equation 3.13 describes the update of each element MD_j $(1 \leq j \leq m)$ of vector MD more formally. After processing each frame of sequence $\{f_1, f_2, f_3, \ldots, f_n\}$ and updating the elements of MD vector accordingly, we classify the sequence as action c which has the smallest value MD_c in MD vector. Equation 3.14 depicts how the final decision is taken in mathematical notation.

$$MD_j = MD_j + \min\ d_j(i,k) \quad \forall k \ 1 \leq k \leq K \tag{3.13}$$

$$\mathbf{arg\ min}_c\ MD_c \quad \forall c \ 1 \leq c \leq m \tag{3.14}$$

3.5.3 Dynamic Time Warping

Both of the previous classification schemes are based on the individual comparison of each frame to key frames extracted for each action. Although they are simple and straightforward to implement, Majority Voting and Sum of Minimum Distances fail to catch the relative ordering of the poses occurred in an action sequence. This drawback may manifest itself in deterioration of the recognition rate when there exists some actions which consist of a set of poses encountered in reverse order in time. As an example we can give sitting down and standing up as a representative pair for these kind of actions.

Dynamic Time Warping (DTW) [23] is a technique that is being extensively used in speech recognition. Taking its power from dynamic programming, DTW compares two series with different sizes by finding an optimal alignment between them. We employ DTW in order to align the poses of two action sequences and find a correspondence between their pose order.

We classify a given action sequence as follows. By means of DTW, we first compare the test sequence $\{f_1, f_2, f_3, \ldots, f_n\}$ with each training sequence $t = \{t_1, t_2, t_3, \ldots, t_l\}$ where l is the length of the training sequence. An important point to emphasize here is that we do not use the training sequence $t = \{t_1, t_2, t_3, \ldots, t_l\}$ as is. Instead, we represent it with a set of key frames of action j which the training sequence belongs to. For example, instead of using t_1 during the comparison, we use key frame KF_{jc} for a particular c $(1 \leq c \leq K)$ which is the most similar key frame to t_1 among all of the key frames in KF_j. After comparing it with the training sequences of all actions, we classify the test sequence as the action which has the training sequence that is most similar to test sequence in DTW distance.

Chapter 4

Experiments

This chapter consists of the experiments that we have conducted to evaluate our action recognition scheme. First, we describe the state of the art action recognition datasets (Section 4.1). Then, we present the results we obtain on these datasets (Section 4.2). Finally, we compare our results with the existing works in the literature (Section 4.3).

4.1 Datasets

4.1.1 Weizmann

Weizmann dataset was introduced by Blank et al. in [9]. It consists of 9 actions such as walk, run, jump, side, bend, wave1 (one-hand wave), wave2 (two-hands wave), pjump (jump in place) and jack. The actions are performed by 9 different actors. There are total of 81 videos in the entire dataset. When testing our approach on Weizmann, we used the silhouette images, which are provided as part of the dataset, for point generation step. We apply leave-one-out classification for all of the experiments performed on this dataset. Figure 4.1 shows the example poses taken from Weizmann dataset.

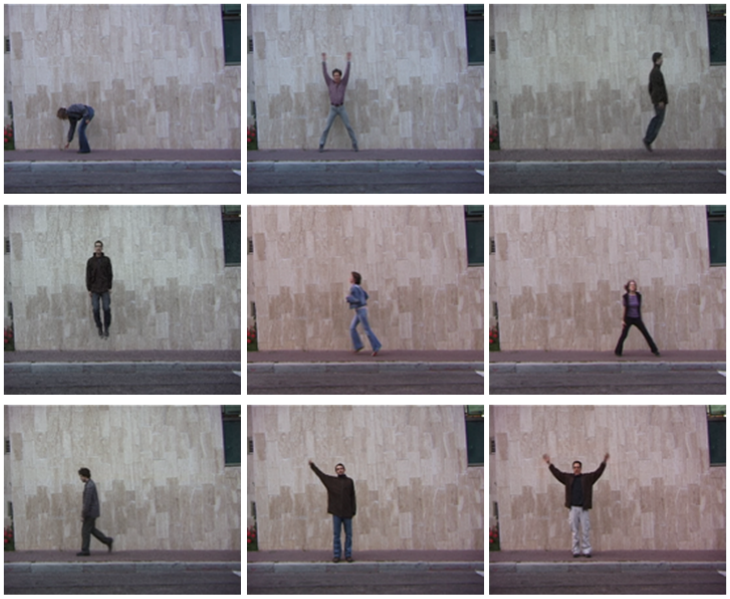

Figure 4.1: This figure shows samples taken from 9 actions in Weizmann dataset. **Top Row:** bend, jack, jump **Middle Row:** pjump, run, side **Bottom Row:** walk, wave1,wave2

4.1.2 KTH

KTH dataset contains 6 actions (boxing, hand-clapping, hand-waving, jogging, running, walking) performed by 25 different actors in 4 scenarios; outdoors (s1), outdoors with changing scale and viewpoints (s2), outdoors with different clothes (s3) and indoors with changing illumination (s4). There are total of 600 videos in the entire dataset. Because of the large number of available frames for each action, the key frame extraction step requires a significant amount of time. For this reason, we split the dataset into two as training and test samples. Moreover, instead of extracting K number of key frames for each action, we extract K number of key frames for each scenario of each action. This leads having a total of $4 \times K$ number of key frames for each action. In KTH dataset, actions are performed with varying periodicity. For consistency, we trim action sequences to 20-50 frames so that the action is performed only once. Figure 4.2 shows the sample frames taken from KTH dataset.

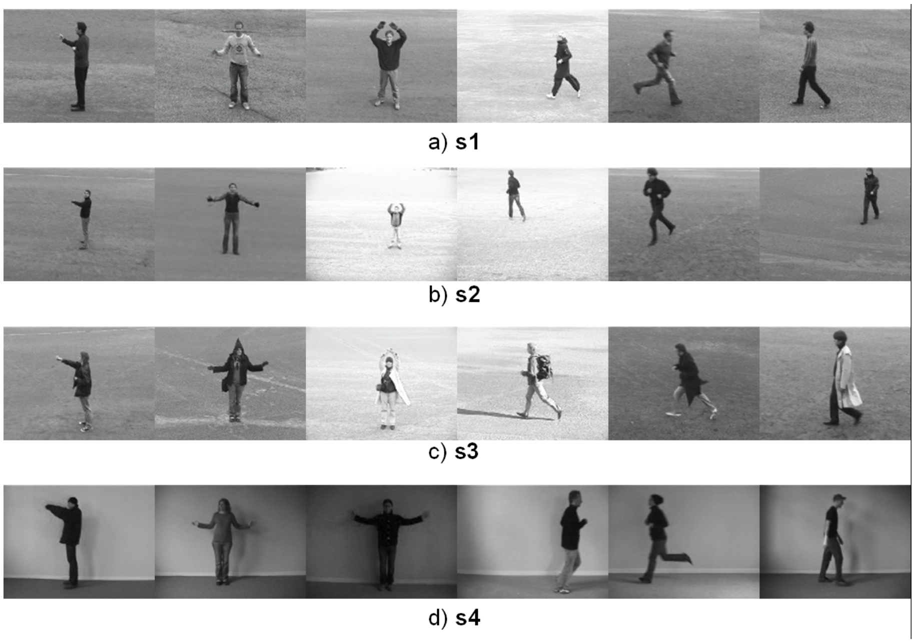

Figure 4.2: This figure shows samples taken from 4 different shooting conditions (s1, s2, s3 and s4) of KTH dataset. Boxing, hand-clapping, hand-waving, jogging, running and walking actions are shown in Column 1 to 6 in the respective order.

4.2 Experimental Results

This section presents the experimental results we obtained by testing our approach on the Weizmann and KTH datasets.

4.2.1 Evaluation of Number of Key Frames

As our first experiment, we show how the number of key frames (K) affects recognition performance. In Section 3.3, we indicated that human brain can recognize an action instantenously just by looking at a single frame. This observation encourages us in using a small number for K in our experiments. Figure 4.3 shows the recognition rate when the number of key frames extracted for each action is 2, 5, 10, 15, 20 and 50. The same figure also demonstrates the effect of spatial binning discussed in Section 3.2.3. Previously, we noted that the spatial binning approach can be generalized into any $N \times N$ binning. For our experiments, we

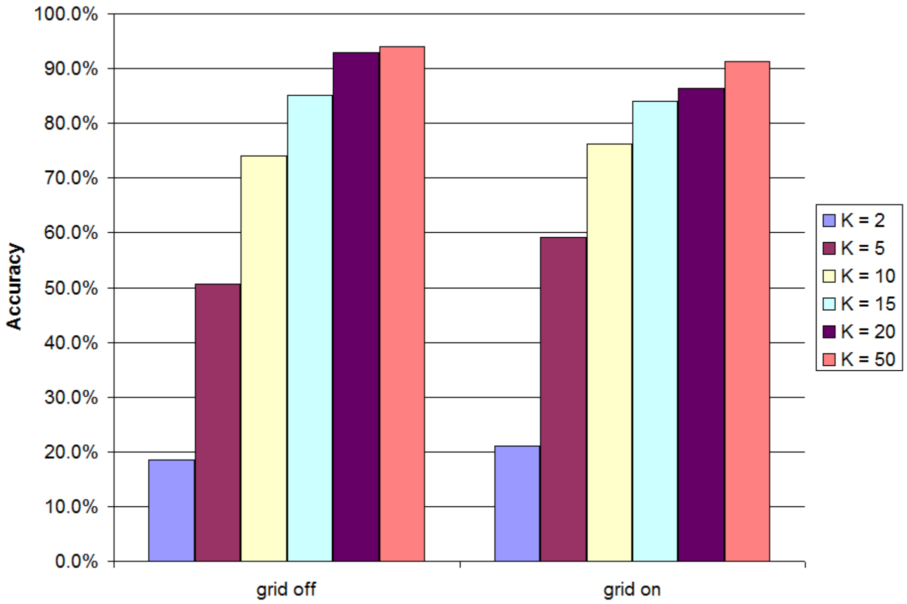

Figure 4.3: This figure illustrates the effect of the number of key frames and spatial binning option on recognition performance. **grid off** and **grid on** labels on x-axis represent the results when the spatial binning option is off and on, respectively.

use N = 2 to show the effectiveness of spatial binning.

As shown in the figure, the highest recognition rates are %93 and %94 and they are obtained when the number of key frames employed to represent each action is 20 and 50, respectively. The most noticeable trend in the results is the large improvement of recognition rate when we increase the number of used key frames from 2 to 5 and from 5 to 10. Once a saturation point is reached in terms of K, increasing it (from 20 to 50) further results in a small step up of the overall performance (from %93 to %94).

Figure 4.4 presents the confusion matrices of the best results in Figure 4.3. Most of the confusion occur among jump-pjump and run-side-walk actions. Since for this experiment we only utilize shape of human pose, it is quite reasonable to have such misclassifications. Jump and pjump are basically variations of the same action (jump is performed with motion towards a certain direction whereas pjump is performed in place). Similarly, run, side and walk actions show quite similar pose appearances and they mostly differ in speed the action is performed.

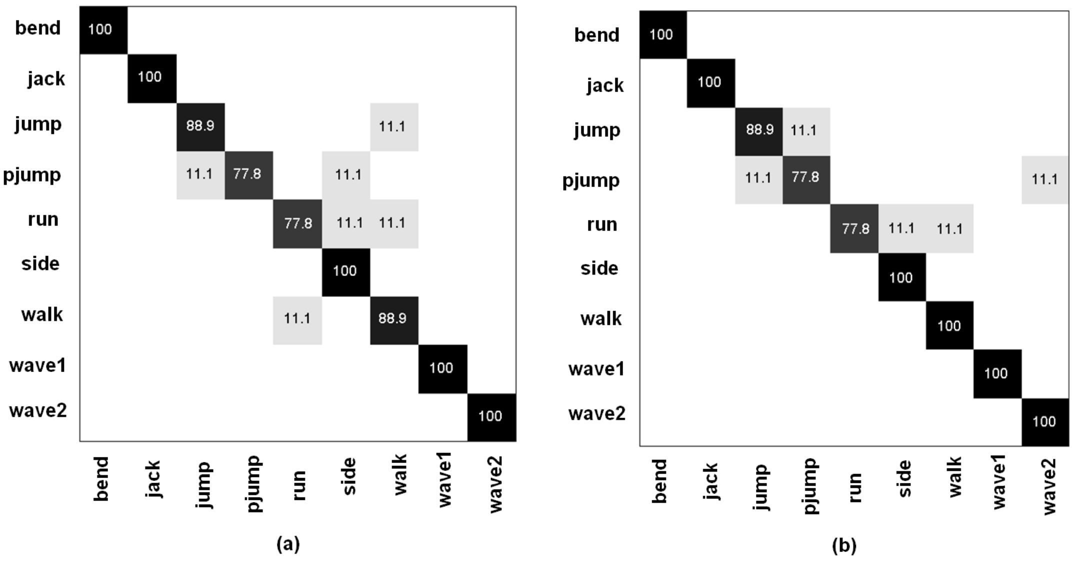

Figure 4.4: This figure shows the confusion matrices of the best results in Figure 4.3. We achieve %93 and %94 accuracy values when K = 20 (given in **(a)**) and K = 50 (given in **(b)**). Most of the confusions occur among jump - pjump and run - side - walk actions.

Introducing a certain level of motion information would resolve these issues.

4.2.2 Evaluation of Spatial Binning and Tolerance

An important observation about the results in Figure 4.3 is the positive effect of spatial binning option upto a certain point. Placing a 2×2 imaginary grid over the human figure and allowing the points to be matched only if they come from the same grid region leads to reasonable jumps in the accuracy (from %50.6 to %59.3 when $K = 10$ and from %74.1 to %76.1 when $K = 15$). However, the results when $K = 15, 20, 50$ and spatial binning turned off overperform the results with the same number of key frames when spatial binning is turned on. As emphasized in Section 3.2.3, we believe that this expected decrease is caused by the imperfections in the boundary coordinates of spatial bin regions for some test sequences. To reduce negative effect of the miscalculations, we introduce a tolerance value which enables the points that fall in two neighbor bin regions to be matched if they

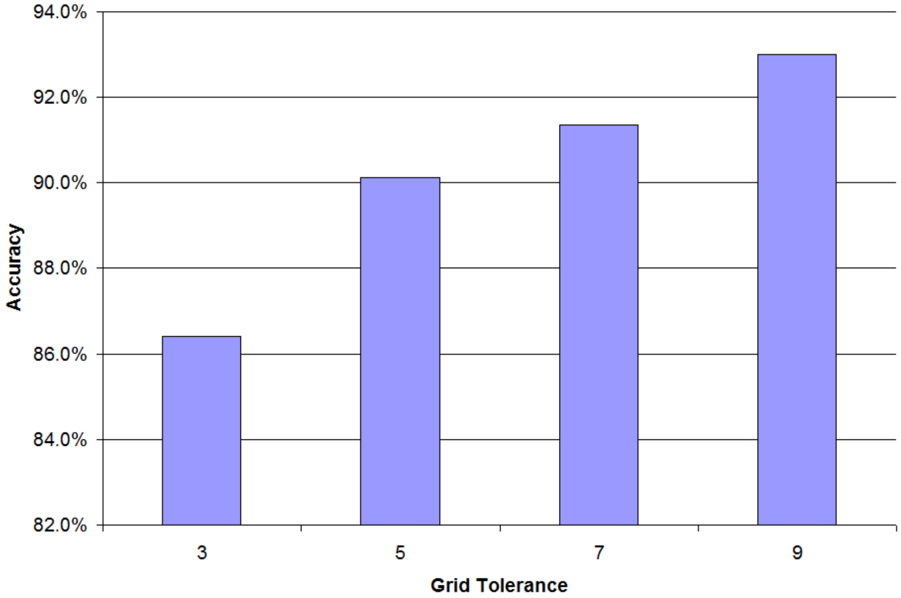

Figure 4.5: This figure illustrates the effect of tolerance on results when spatial binning is turned on. Tolerance value is defined in pixel units. (3 pixels, 5 pixels, 7 pixels and 9 pixels)

are located within a certain distance to the boundary between those regions. Figure 4.5 shows the effect of *tolerance* value on recognition performance when repeating the experiment in Figure 4.3 with $tolerance = 3, 5, 7, 9$ and $K = 20$. Increasing tolerance value from 3 to 9 provides a considerable elevation (%7) and provides the same recognition rate %93 as its counterpart when spatial binning is disabled. Defining a tolerance value gives us a more flexible version of original spatial binning constraint. Moreover, it clearly provides a better recognition performance for all K when compared to the results where no spatial binning constraint is enforced.

4.2.3 Adjusting Sampling Factor for Point Generation

In Section 3.1.3, we emphasized the importance of feeding the shape context algorithm with a good set of points for the accurate representation of the pose in a given frame. As the number of points sampled from human contour increases,

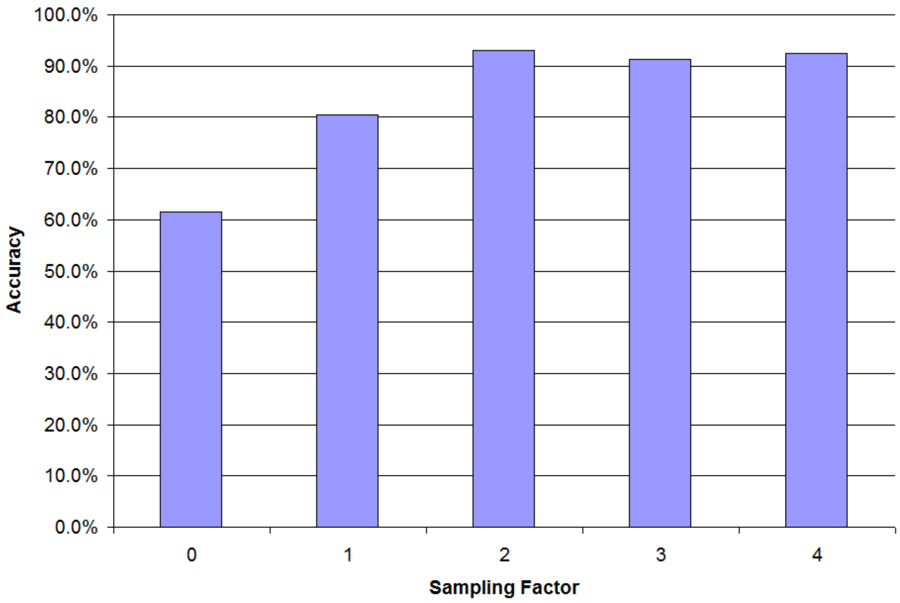

Figure 4.6: This figure shows the effect of sampling factor s used in point generation. As the sampling factor gets larger, the recognition rate improves to a certain point and then fluctuates slightly within a certain band of accuracy.

shape context gets better in fetching the shape formed by the human pose. Figure 4.6 illustrates the effect of sampling factor s we use for point generation on recognition accuracy. When sampling factor s is 0, we only utilize the center points of the extracted lines as sampled points. As the figure clearly shows, using only center points is not enough for good classification. The big jump in recognition rate (from %61.5 to %93.1) after setting sampling factor to 1 is a strong indication of sampling factor being a crucial parameter.

4.2.4 Evaluation of Different Classification Techniques

For recognizing actions, we utilize four different classification schemes; Majority Voting with 1-NN, Majority Voting with 3-NN, Sum of Minimum Distances and Dynamic Time Warping. The first three schemes can be described as having similar natures since all three of them are based on individual comparison of each frame to key frames of all actions. On the other hand, aligning two pose sequences and finding the best possible pose order between them, Dynamic Time Warping

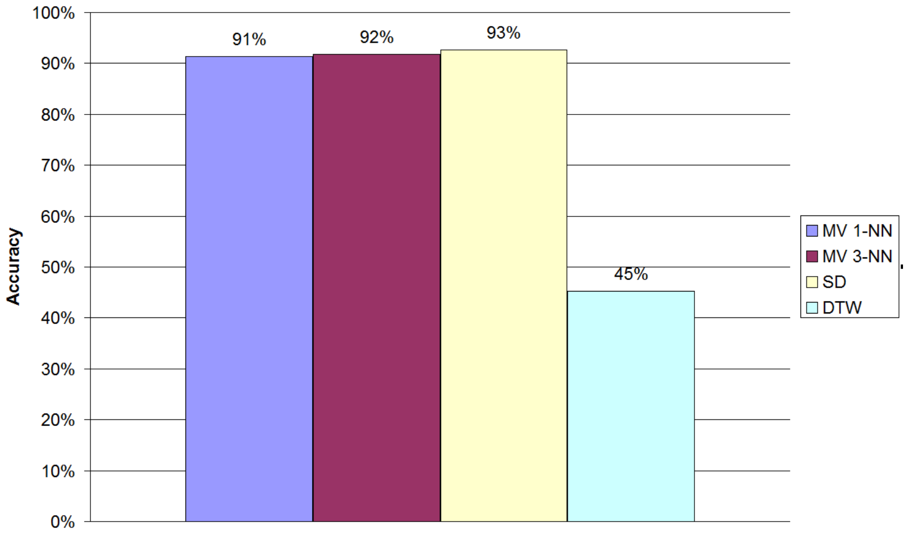

Figure 4.7: This figure illustrates the recognition accuracies provided by each classification method. In the figure, MV 1-NN, MV 3-NN, SD and DTW stand for Majority Voting with 1-NN, Majority Voting with 3-NN, Sum of Minimum Distances and Dynamic Time Warping, respectively.

provides a different recognition alternative. Figure 4.7 shows the performances of each scheme in an experiment on Weizmann dataset, where the number of key frames K for each action is 40 with spatial binning option turned off. As expected, the first three methods (MV 1-NN, MV 3-NN and SD) are able to recognize almost the same amount of samples and present recognition rates between %91 and %93. Surprisingly, DTW appears as the worst classifier and remains at merely %50 accuracy. From these observations, we can conclude that Dynamic Time Warping is not suitable to be used along with a key frame based action recognition approach. For the rest of the experiments, we drop DTW and utilize MV 1-NN, MV 3-NN and SD as our classifiers.

4.2.5 Evaluation of Matching Methods

In Section 3.2.1, we present two point matching techniques Left-To-Right Matching (LRM) and Hungarian Method which are used to find a matching between the point sets of a given pair of frames. Looking at different perspectives, these two matching methods provide different strategies. LRM tries to match each

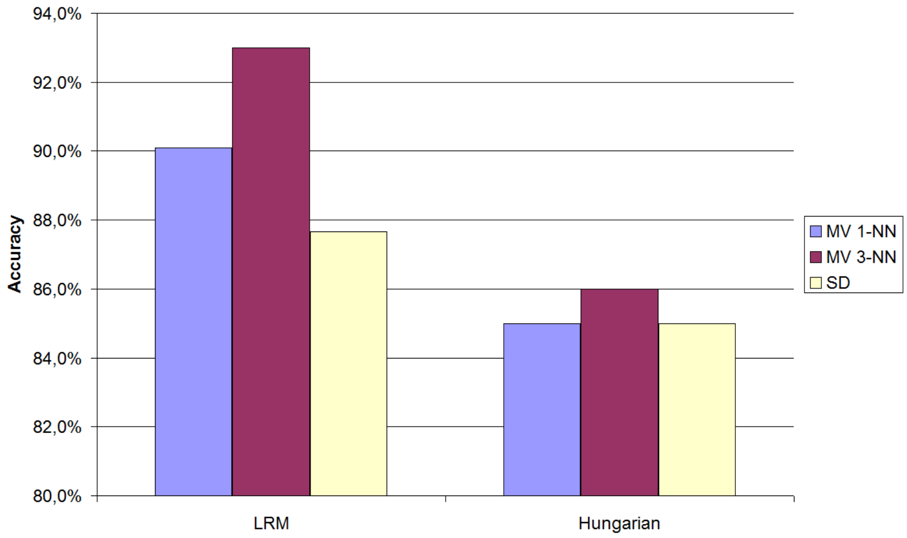

Figure 4.8: This figure demonstrates how using Left-To-Right Matching (LRM) or Hungarian Method affects the recognition performance. LRM provides a %93 recognition rate whereas Hungarian Method remains at %86

.

point in first frame to the most similar point in second frame, but it does not necessarily provide a match for each and every point. On the other hand, providing a match for each point, Hungarian Method seeks to minimize summation of individual similarities by avoiding to match the closest points right away. Figure 4.8 shows that using Left-To-Right Matching (LRM) overperforms Hungarian Method. This observation is important since it is an indication of Hungarian Method not being applicable to human action recognition as a point matching technique to define the similarity between two human poses. Although Belongie et al. in [1] suggest Hungarian Method when using Shape Context Descriptor, LRM is more successful in analysing similarities and dissimilarities of a given pair of human pose. Moreover, Hungarian Method, which is essentially a combinatorial optimization algorithm, takes a considerable time when looking for global optimum. For the rest of the experiments, we do not test Hungarian Method and utilize Left-To-Right Matching as our point matching scheme.

4.2.6 Utilizing Other Visual Clues

It is desirable to use other visual clues such as image appearance in combination with Shape Context Descriptor when defining a similarity value between two points. As we emphasized in Section 3.2.2, these individual distances can be summed up by a weigted manner and similarity matrix between points can be generated accordingly. With Formula 3.5, we defined a distance which measures the similarity of two points in terms of orientation of the lines that the points are originated from. Our results show that none of different weight sets ($\alpha_{sc}, \alpha_\theta$) that we give to each similarity value (shape context distance and orientation distance) improves our previous results. In fact, increasing the effect of orientation distance may sometimes result in the deterioration of recognition performance. We believe that involving the other line characteristics such as line length in Formula 3.5 may give us the improvement we seek for. We leave the exploration of such supplemental line features as a future work.

4.2.7 Involving Motion Information

In Section 3.4, we explained how we can introduce a level of motion information to the key frame selection process. We described how we compute two displacement vectors referred as “from where” and “to where” for each frame in a sequence. As mentioned previously, there are two ways to integrate the motion information. One way is to calculate the distance between displacement vectors of two frames and to add the resulting value as a constant to shape context similarity values of points at the beginning of point matching. This method is desribed by Formula 3.9. Alternatively, after point matching is done, we can add the same values to the distance between two frames as depicted in Formula 3.10. In our experiments, we observed that the first alternative does not give us the performance improvement we seek for. Thus, in this section, we only focus on the second alternative.

Figure 4.9 illustrates the effect of using motion information on Weizmann dataset. As we expected, we obtained a %4-5 increase in performance and achieved a %98 accuracy when the number of key frames K for each action was

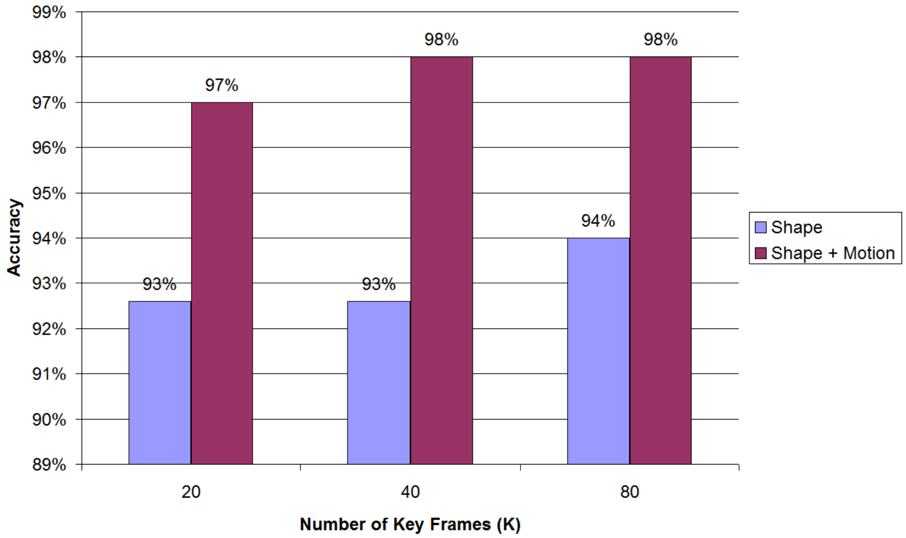

Figure 4.9: This figure illustrates the effect of using Motion information along with Shape on Weizmann dataset. When the number of key frames K for each action is 80, we obtained a %98 accuracy.

80. Figure 4.10 presents the confusion matrix of the same result. As it can be seen, the only confusions occur between pjump-wave1 and run-walk. This result seems quite reasonable since pjump and wave1 actions only differ by a single hand in shape. Besides this confusion, the same up and down movement of the points in their poses is another factor which makes them hard to be distinguished by our displacement vectors. Moreover, the second confusion between run and walk sequence might be a good indication of the need to use a global motion information.

Figure 4.11 shows the performance of using only shape information and using shape and motion information together on KTH dataset. Our approach without using motion information achieves a %77 recognition rate when the number of key frames we extracted for each action is 120 (30 key frames for each scenario for each action). When involving motion information, we obtain %4 improvement and achieve %81 accuracy. In this result, the individual performance values obtained for each shooting scenario are %92 for SC1, %64 for SC2, %85 for SC3 and %79 for SC4. SC2 videos are shot in presence of scale and viewpoint variations leading to a considerably large number of possible pose appearances for each action.

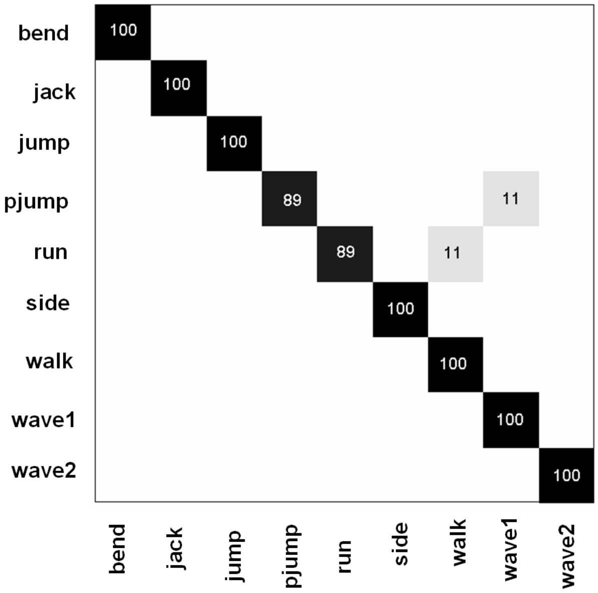

	bend	jack	jump	pjump	run	side	walk	wave1	wave2
bend	100								
jack		100							
jump			100						
pjump				89				11	
run					89		11		
side						100			
walk							100		
wave1								100	
wave2									100

Figure 4.10: This figure shows the confusion matrix for the best result in Figure 4.9

.

Therefore, SC2 appears as the shooting condition where our approach works the worst. Here, increasing the number of poses should increase the performance upto a certain point. However, increasing K further also increases the required time for the classification step. Figure 4.12 presents the confusion matrix for the best result in Figure 4.11. Generally, the confusions occur among two groups; boxing-handclapping-handwaving and jogging-running-waving. Especially, the failure in recognizing running action stands as a striking observation. Again, this observation is another clear indication of the absolute need in utilizing a global motion feature.

We believe that the results we obtained on this dataset are acceptable since KTH is quite a challenging dataset with different shooting conditions. Moreover, because of time concerns we split this dataset as testing and training, but it is known that applying leave-one-out cross validation may provide performance improvements upto %10.

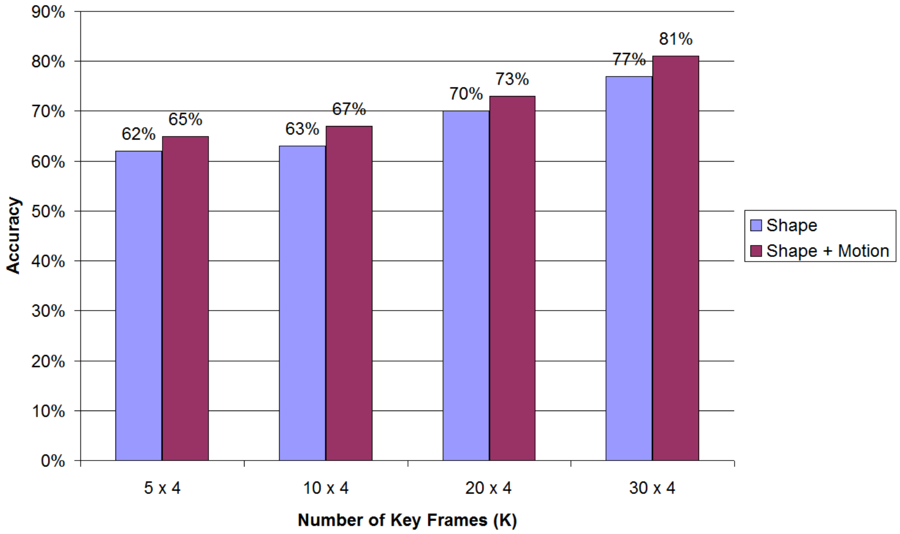

Figure 4.11: This figure illustrates the effect of using Motion information along with Shape on KTH dataset. When the number of key frames K for each action is 120 (30×4), we obtained a %81 accuracy.

.

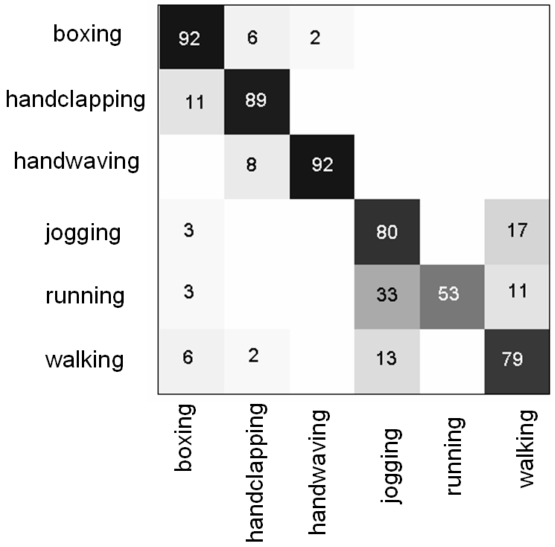

	boxing	handclapping	handwaving	jogging	running	walking
boxing	92	6	2			
handclapping	11	89				
handwaving		8	92			
jogging	3			80		17
running	3			33	53	11
walking	6	2		13		79

Figure 4.12: This figure shows the confusion matrix for the best result in Figure 4.11

.

4.3 Comparison to Related Studies

In this thesis, our first goal was to present a new representation that combines shape and motion information in an action sequence within a key frame based approach. Most of the recent approaches have perfect recognition rates (%100) on Weizmann dataset. Although we achieved %98 accuracy on this dataset, we were unable to classify only 2 sequences out of 81 and we managed to get better results compared to the studies in [20] (%73) and [27] (%87). In KTH dataset, the performance values previous studies achieve range from %73 [25] to %95 [16]. Using a split-based testing method, our approach achieves a %81 accuracy and performs better than the studies in [13] (%80), [18] (%73) and [25] (%72).

Chapter 5

Conclusion

5.1 Summary and Discussion

In this thesis, we present an action recognition approach that is based on a number of stored pose prototypes ("key frames") for each action. To describe the human pose represented in a frame, we use the well-known Shape Context Descriptor which is generally employed for object recognition purposes. We compare the shapes of the poses in a given pair of frames by means of Shape Context Descriptor. During the shape comparison phase, we also utilize simple displacement vectors ("from where" and "to where") that we compute for each frame and introduce a level of motion information to the key frame selection process. As a final step, grouping the frames into a predefined number of clusters provides us a set of key frames for each action which makes it easier to distinguish that specific action from the rest of the action set.

For classifying a given sequence of poses, we utilize three schemes; Majority Voting, Sum of Minimum Distance and Dynamic Time Warping. Majority Voting and Sum of Minimum Distances can be categorized as frame-by-frame comparison schemes and they are simple and powerful enough to find the most similar action to a given pose sequence. On the other hand, Dynamic Time Warping, which finds a correspondence between the pose order of two action sequences, can also be utilized as an alternative classification scheme.

The experiments we have conducted on Weizmann and KTH datasets show that Shape Context is a powerful shape descriptor and it is efficient to grasp the nature of the poses formed by the human figure during the time an action is performed. Moreover, on top of describing the shapes by Shape Context, employing a set of frames as “key frames” is indeed desirable compared to using whole sequences in training samples. Moreover, our results indicate that even simple displacement vectors for motion can eliminate shortcomings of merely using the human pose and elevate recognition accuracy considerably.

5.2 Future Work

Classification performance of our approach presented in this thesis mostly depends on the step in which we group the similar frames of an action into a predefined number of clusters. Measuring how well the frames of an action are grouped appears as the preferred work for future research. Evaluation of clusters by existing Data Mining techniques and reassigning frames into clusters if necessary may lead to significant increases in recognition accuracy. Our experimental work shows that utilizing the local motion information present in a frame boosts up performance to a certain point. Yet still, employing some features that reflects the global motion information in the sequence is desirable. Therefore, inspecting the motion in each frame and generating a general displacement vector for the entire sequence stands as a second future work. When calculating similarity between two points, combining Shape Context distance with orientation distance in weighted fashion does not elevate recognition performance. We will modify the orientation distance in a way such that it reflects other line characteristics such as length as well. As a last future work, we plan on letting each classification technique take a role in the overall decision process. Although the individual performance of Dynamic Time Warping is far from being acceptable, we believe that combining Majority Voting or Sum of Minimum Distances with Dynamic Time Warping would give us a more powerful classifier.

Bibliography

[1] S. Belongie, J. Malik, and J. Puzicha. Shape context: A new descriptor for shape matching and object recognition. *NIPS*, pages 831–837, 2000.

[2] M. Blank, L. Gorelick, E. Shechtman, M. Irani, and R. Basri. Actions as space-time shapes. *ICCV*, 2005.

[3] A. F. Bobick and J. W. Davis. The recognition of human motion using temporal templates. *Pattern Analysis and Machine Intelligence*, 23:257–267, 2001.

[4] S. Carlsson and J. Sullivan. Action recognition by shape matching to key frames. *Workshop on Models versus Exemplars in Computer Vision*, 2001.

[5] P. Dollar, V. Rabaud, G. Cottrell, and S. Belongie. Behavior recognition via sparse spatio-temporal features. *VS-PETS*, 2005.

[6] A. A. Efros, A. C. Berg, G. Mori, and J. Malik. Recognizing action at a distance. *ICCV*, 2003.

[7] A. Fathi and G. Mori. Action recognition by learning mid-level motion features. *CVPR*, 2008.

[8] V. Ferrari, L. Fevrier, F. Jurie, and C. Schmid. Groups of adjacent contour segments for object detection. *IEEE Trans. Pattern Anal. Mach. Intel l.*, 30:36–51, 2008.

[9] L. Gorelick, M. Blank, E. Shechtman, M. Irani, and R. Basri. Actions as space-time shapes. *ICCV*, 2005.

[10] K. Hatun and P. Duygulu. Pose sentences: a new representation for action recognition using sequence of pose words. *ICPR*, 2008.

[11] N. Ikizler, R. G. Cinbis, and P. Duygulu. Human action recognition with line and flow histograms. *ICPR*, 2008.

[12] N. Ikizler and P. Duygulu. Human action recognition using distribution of oriented rectangular patches. *Image and Vision Computing*, 27, 2009.

[13] Y. Ke, R. Sukthankar, and M. Hebert. Spatio-temporal shape and flow correlation for action recognition. *Visual Surveillance Workshop*, 2007.

[14] H. W. Kuhn. The hungarian method for the assignment problem. *Naval Research Logistics Quarterly*, 2:83–97, 1955.

[15] I. Laptev, M. Marszalek, C. Schmid, and B. Rozenfeld. Learning realistic human actions from movies. *CVPR*, 2008.

[16] Z. Lin, Z. Jiang, and L. S. Davis. Recognizing actions by shape-motion prototype trees. *ICCV*, 2009.

[17] J. Liu and M. Shah. Learning human actions via information maximization. *CVPR*, 2008.

[18] J. Liu, J. Yang, Y. Zhang, and X. He. Action recognition by multiple features and hyper-sphere multi-class svm. *ICPR*, 2010.

[19] G. Loy, J. Sullivan, and S. Carlsson. Pose based clustering in action sequences. *Workshop on Higher-Level Knowledge in 3D Modeling and Motion Analysis*, 2003.

[20] J. C. Niebles, H. Wang, and L. Fei-Fei. Unsupervised learning of human action categories using spatial-temporal words. *International Journal of Computer Vision, 79(3):299-318*, 2008.

[21] S. Nowozin, G. Bakir, and K. Tsuda. Discriminative subsequence mining for action classication. *ICCV*, 2007.

[22] H. Qu, L. Wang, and C. Leckie. Action recognition using space-time shape difference images. *ICPR*, 2010.

[23] L. Rabiner and B. Juang. Fundamentals of speech recognition. 1993.

[24] K. Schindler and L. V. Gool. Action snippets: how many frames does human action recognition require? *CVPR*, 2008.

[25] C. Schuldt, I. Laptev, and B. Caputo. Recognizing human actions: a local svm approach. *ICPR*, 2004.

[26] C. Thurau and V. Hlavac. Pose primitive based human action recognition in videos or still images. *CVPR*, 2008.

[27] C. Thurau and V. Hlavac. Pose primitive based human action recognition in videos or still images. *CVPR*, 2008.

[28] Y. Wang, P. Sabzmeydani, and G. Mori. Semi-latent dirichlet allocation: a hierarchical model for human action recognition. *ICCV Workshop on Human Motion*, 2007.